Crystal field ground state of the orthorhombic Kondo semiconductors $CeOs_2Al_{10}$ and $CeFe_2Al_{10}$

F. Strigari,[1] T. Willers,[1] Y. Muro,[2] K. Yutani,[2] T. Takabatake,[2,3] Z. Hu,[4] S. Agrestini,[4] C.-Y. Kuo,[4] Y.-Y. Chin,[5] H.-J. Lin,[5] T. W. Pi,[5] C. T. Chen,[5] E. Weschke,[6] E. Schierle,[6] A. Tanaka,[2] M. W. Haverkort,[7,8] L. H. Tjeng,[4] and A. Severing[1]

[1]*Institute of Physics II, University of Cologne, Zülpicher Straße 77, 50937 Cologne, Germany*
[2]*Department of Quantum Matter, AdSM, Hiroshima University, Higashi-Hiroshima 739-8530, Japan*
[3]*Institute for Advanced Materials Research, Hiroshima University, Higashi-Hiroshima 739-8530, Japan*
[4]*Max Planck Institute for Chemical Physics of Solids, Nöthnizer Straße 40, 01187 Dresden, Germany*
[5]*National Synchrotron Radiation Research Center (NSRRC), 101 Hsin-Ann Road, Hsinchu 30077, Taiwan*
[6]*Helmholtz-Zentrum Berlin für Materialien und Energie, Albert-Einstein-Straße 15, 12489 Berlin, Germany*
[7]*Max Planck Institute for Solid State Research, 70569 Stuttgart, Germany*
[8]*Department of Physics and Astronomy, University of British Columbia, Vancouver, Canada V6T1Z1*

(Received 22 October 2012; published 14 March 2013; corrected 20 March 2013)

Here we present linear-polarization-dependent soft x-ray absorption spectroscopy data at the Ce $M_{4,5}$ edges of $CeOs_2Al_{10}$ and $CeFe_2Al_{10}$. Despite the strong hybridization between $4f$ and conduction electrons and the existence of spin gaps as seen in inelastic neutron scattering, we were able to determine the crystal field ground state wave functions by combining our spectroscopy data with magnetization measurements. The results quantitatively explain the small ordered moment along c and the measured magnetic moment along the easy a axis in $CeOs_2Al_{10}$.

DOI: 10.1103/PhysRevB.87.125119 PACS number(s): 71.27.+a, 75.10.Dg, 75.30.Cr, 78.70.Dm

Among the strongly correlated electron systems, the Ce-based intermetallic compounds are known to possess many interesting and anomalous phenomena. The CeM_2Al_{10} compounds with M = Ru, Os, and Fe belong to a fairly new family of cerium Kondo semiconductors which gained considerable prominence for their unusual high magnetic ordering temperatures of $T_0 = 27$ K ($CeRu_2Al_{10}$) and 29 K ($CeOs_2Al_{10}$).[1,2] This novel phase transition is, for example, observed in the electrical resistivity, the specific heat, and the magnetization, and several scenarios have been discussed to explain the origin of the magnetic order.[1–26] Isostructural $CeFe_2Al_{10}$ lacks any phase transition and shows the highest degree of hybridization between $4f$ and conduction electrons (c-f hybridization) within the family.[2,27–32]

The static magnetic susceptibility of these orthorhombic compounds (space group $Cmcm$) is very anisotropic with $\chi_a > \chi_c > \chi_b$.[2,5,6,19,32] This is mainly due to crystalline electric field (CEF) effects. The susceptibility along the b and c axis is only weakly temperature dependent in all three composites. The temperature dependence of the susceptibility along the easy a axis shows that the Kondo effect becomes more pronounced from M = Ru to Os to Fe: In $CeRu_2Al_{10}$ χ_a is Curie-Weiss-like and drops sharply at the ordering transition at 27 K, whereas in $CeOs_2Al_{10}$ and $CeFe_2Al_{10}$ it undergoes a broad maximum at $T_{max} \approx 45$ and 70 K, respectively, and shows enhanced Pauli paramagnetism at low temperatures. The absolute magnitude of χ_a and χ_c in $CeFe_2Al_{10}$ is about half as much as in the Ru and Os compound. $CeFe_2Al_{10}$ is therefore classified as an intermediate valence system.[27]

Inelastic neutron scattering (INS) experiments have found spin gaps of 8 meV (Ru) and 11 meV (Os) in the ordered state.[9,11] The long-range nature of the antiferromagnetic order in the Ru and Os compound has been confirmed by μSR and neutron diffraction experiments. However, the mechanism of the ordering remains puzzling,[4,9–11,17,18] because the Ce-Ce distances of more than 5 Å in the cagelike crystal structure[33,34] are very large and it is not easy to understand quantitatively the high ordering temperatures in the context of Ruderman-Kittel-Kasuya-Yosida exchange interactions. Further, the ordering temperatures are too high according to the de Gennes scaling from the Gd equivalents.[2]

In CeM_2Al_{10} the $J = 5/2$ and $7/2$ multiplets of Ce^{3+} split into seven Kramer's doublets under the influence of an orthorhombic crystal field (point group C_{2v}). In the basis of $|J, J_z\rangle$ each of these states has the general form

$$\sum_{J_z=-5/2,-3/2,\ldots,5/2} \alpha_{J_z}|5/2, J_z\rangle + \sum_{J_z=-7/2,-5/2,\ldots,7/2} \beta_{J_z}|7/2, J_z\rangle \quad (1)$$

for values of J_z which fulfill $\sum_{J_z}(\alpha^2_{J_z} + \beta^2_{J_z}) = 1$ and $\Delta J_z = \pm 2$. The CEF ground state (GS) wave function of the $4f$ electrons in $CeRu_2Al_{10}$ has been successfully determined in a previous study.[35] In the present work the investigation of the crystal field GS is extended to the other two members of the compound family. The $4f$ GS wave functions are expected to be highly anisotropic due to the presence of the CEF in the orthorhombic $YbFe_2Al_{10}$-type structure. The importance of CEF effects on ground state properties has been discussed in Ref. 35 (and references therein). As shown for the case of $CeRu_2Al_{10}$, linearly polarized x-ray absorption spectroscopy (XAS) at the Ce $M_{4,5}$ edge is a powerful technique for determining CEF GS wave functions in orthorhombic Kondo semiconductors with spin gaps. The selection rules of linear polarized light yield the sensitivity to the initial state symmetry.

Single crystals of $CeOs_2Al_{10}$ and $CeFe_2Al_{10}$ were grown by an Al self-flux method[5,32] and their quality and orientation were confirmed by Laue x-ray diffraction. The XAS measurements were carried out at the synchrotron light sources BESSY II of the Helmholtz-Zentrum Berlin in Germany (undulator beamline UE46-PGM1) and the National Synchrotron Radiation Research Center (NSRRC) in Taiwan (Dragon bending magnet beamlines BL08A1 and BL11A1). The energy resolution at the Ce $M_{4,5}$ edge ($h\nu \approx 870$–910 eV) was about

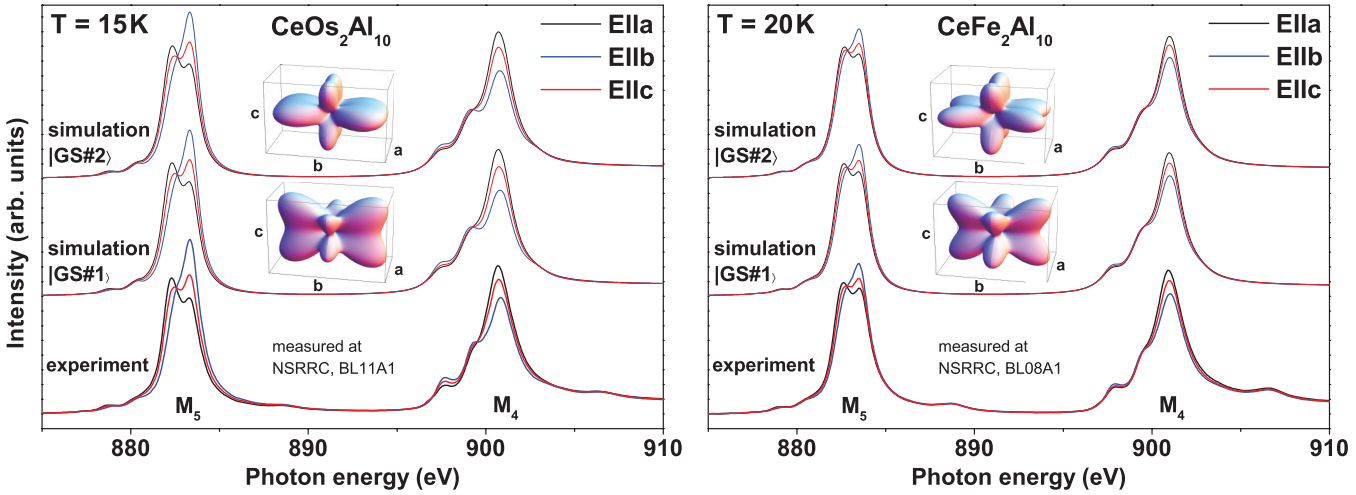

FIG. 1. (Color online) Experimental low-temperature linearly polarized soft x-ray absorption data of $CeOs_2Al_{10}$ (bottom curves in the left panel) and $CeFe_2Al_{10}$ (bottom curves in the right panel) at the $M_{4,5}$ absorption edge. The middle and top set of spectra in each panel represent the two simulations which reproduce the experimental data. For both CEF ground states, $|GS\#1\rangle$ and $|GS\#2\rangle$, the corresponding spatial distributions of the $4f$ electrons are included as insets.

0.15 eV (BESSY II) and 0.4 eV (NSRRC) and the crystals were cleaved *in situ* in a vacuum of $\sim 10^{-10}$ mbar. Further details about the technical conditions and measurement procedure can be found in Ref. 35.

In cerium heavy fermion/Kondo compounds, where the well-localized $4f$ electrons hybridize with the conduction electrons, the ground (initial) state is a mixture of the configurations $4f^0$, $4f^1$, and $4f^2$.[36,37] However, typically the spectral weights in the XAS M edges due to the $4f^0$ and $4f^2$ initial configurations are minor with respect to $4f^1$ (see below) and the $3d \rightarrow 4f$ absorption is well characterized by atomiclike transitions into multiplet-split final states.[36] We therefore performed the same ionic full multiplet simulations for the data analysis as for $CeRu_2Al_{10}$ (Ref. 35) using the XTLS 8.3 program.[38] Reference 39 points out why for crystal-field purposes the ionic approach is preferable over the Anderson impurity model as long as the crystal-field splittings are large with respect to the Kondo temperature—something still valid for the two compounds under investigation in this work. Our ionic calculations comprise the intra-atomic $4f$-$4f$ and $3d$-$4f$ Coulomb interactions, the $3d$ and $4f$ spin-orbit coupling, and the CEF parameters, which reflect the full symmetry of the ligand field surrounding the Ce ion. Hybridization or band effects are not included.

For the simulations the atomic parameters are adjusted at first, i.e., the Hartree-Fock values were reduced to reproduce the experimental isotropic spectra $I_{\text{isotropic}} = I_{E\|a} + I_{E\|b} + I_{E\|c}$. The reduction amounts to about 40% for the $4f$-$4f$ and to about 20% for the $3d$-$4f$ Coulomb interactions and accounts for the configuration interaction effects not included in the Hartree-Fock scheme. Subsequently, we used the coherent approach as described in Ref. 35 to simulate the low-temperature XAS spectra, i.e., the relative size of the CEF parameters was varied to reproduce the anisotropy of the XAS data. It should be noted that for the CEF GS wave function only the *relative* size of the CEF parameters matters as long as the CEF energy splitting is small enough with respect to the spin-orbit splitting ($\Delta E_{\text{SO}} = 280$ meV). The *absolute* size of the CEF parameters determines the size of the CEF splittings, which here only enter via thermal population when simulating the temperature evolution of the linear polarization [linear dichroism (LD)]. For the simulation of the CEF-only static susceptibility for $CeOs_2Al_{10}$ we assumed energy splittings of $\Delta E_1 \approx 38$ meV and $\Delta E_2 \approx 63$ meV between the GS and the first and second excited CEF doublet, respectively, and for $CeFe_2Al_{10}$ a quasiquartet at about 51 meV. These numbers are based on INS data by Adroja *et al.*[40]

In Fig. 1 the low-temperature linearly polarized XAS spectra of $CeOs_2Al_{10}$ and $CeFe_2Al_{10}$ are shown (bottom curves in the left and right panels). Due to the orthorhombic point symmetry of cerium in these compounds all three polarizations, i.e., for the incoming light-polarized $E\|a$, $E\|b$, and $E\|c$, were measured.[35] We know that at 15 and 20 K only the ground state is probed, because INS finds CEF excitations above 30 meV energy transfer.[40] Both compounds exhibit a strong polarization effect which can be simulated with the full multiplet routine. As for $CeRu_2Al_{10}$ there are only two solutions describing the threefold anisotropy of the measured low-temperature linearly polarized XAS spectra,[41] which in the following are referred to as $|GS\#1\rangle$ and $|GS\#2\rangle$. Both solutions are mainly composed of the $J = 5/2$ multiplet. Some minor admixtures come from the higher $J = 7/2$ multiplet, however, their effect on the LD is negligible and cannot be seen in the spectra when changing into Stevens approximation.[35] The respective $4f$ orbitals for the solutions $|GS\#1\rangle$ and $|GS\#2\rangle$ are shown as insets. In the dipole limit the two $4f$ distributions look the same so that a technique which is governed by dipole transitions—such as XAS—yields identical spectra for both orbitals.

We follow the same path as in $CeRu_2Al_{10}$ and are able to discard one solution ($|GS\#2\rangle$) by calculating the temperature dependence of the static susceptibility at $H = 1$ T in all three crystallographic directions and compare it to the experimental results found by Muro *et al.*[5,32] The simulations for the $|GS\#1\rangle$

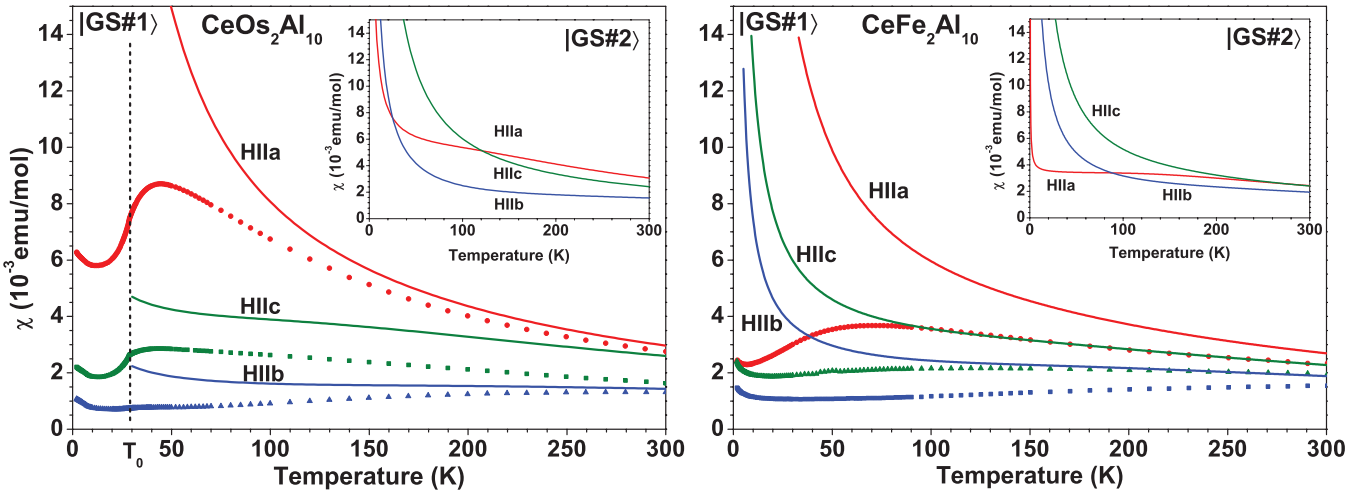

FIG. 2. (Color online) Temperature dependence of the static susceptibility adapted from Refs. 5 and 32 (symbols) and calculated from the two CEF models |GS#1⟩ (lines in main panel) and |GS#2⟩ (lines in insets).

scenario are plotted in the main panel of Fig. 2 (lines) together with the data points taken from Refs. 5 and 32. The simulations for the |GS#2⟩ model are included as an inset. For $CeOs_2Al_{10}$ the |GS#1⟩ scenario reproduces nicely the anisotropy and the qualitative temperature evolution for $T > T_0$. This is not the case for the CEF model based on |GS#2⟩. It yields a crossover of $\chi^a_{\rm CEF}$ and $\chi^c_{\rm CEF}$ at about 120 K and does not match the measured susceptibility. We therefore exclude it as a possible GS wave function. For $CeFe_2Al_{10}$ the general anisotropy is also reproduced by the |GS#1⟩ scenario, whereas the |GS#2⟩ model produces intersections between $\chi^a_{\rm CEF}$ and the susceptibilities along the other two axes. The remaining discrepancy between the measured and CEF-only susceptibility |GS#1⟩ in Fig. 2 can be reduced by considering corrections due to molecular and/or exchange fields and anisotropic hybridization effects. Such an anisotropic c-f hybridization has indeed been observed in optical conductivity measurements[14,21,31] and also the anisotropic spin dynamics as observed in INS on $CeRu_2Al_{10}$ point in this direction.[26] These anisotropic Kondo interactions will affect the anisotropy of the static susceptibility more, the stronger the Kondo effect is. Hence it is not surprising that for $CeFe_2Al_{10}$ the discrepancy between the calculated CEF-only susceptibility based on the |GS#1⟩ scenario is larger than in the Os and Ru (Ref. 35) samples. This goes along with Hanzawa's findings for the Ru and Os compound that including $4f$-$5d$ mixing improves the agreement between calculated and measured susceptibility, and with his suggestion that in the Fe sample this intermixing is so large that the magnetic order is suppressed.[15]

Using the c axis as the quantization axis, the corresponding J_z coefficients of solution |GS#1⟩ are as listed in Table I. We find a very strong $|5/2,\mp 3/2\rangle$ contribution for both compounds which is in agreement with susceptibility simulations by Yutani *et al.*[19] and theoretical studies by Hanzawa, who determined the $4f$ level structure of $CeOs_2Al_{10}$ in a point-charge model.[15] Assuming the CEF splittings mentioned above, we obtain the CEF parameters as summarized in Table II.

The CEF ground-state wave function |GS#1⟩ yields the magnetic moments $\mu^{a,b,c}_{\rm CEF} = (1.35,0.27,0.30)\mu_B$ and $(1.02,0.39,0.53)\mu_B$ for the Os and Fe samples, respectively. An infinitesimal small temperature and magnetic field along the respective crystallographic axes have been used to obtain these values within a single ion CEF calculation. For $CeOs_2Al_{10}$ these CEF-only moments satisfactorily agree with the moment along the easy a axis as found in high field magnetization measurements, $\mu^a_{H=55\,\rm T} \approx 0.95\mu_B$,[16] and the ordered magnetic moment along c determined with neutron diffraction and μSR, $\mu^c_{\rm ord} = 0.20\mu_B$.[11] For the Fe compound there are no values of the moments available from other techniques.

Figure 3 shows the experimental low-temperature isotropic spectra, constructed from $I_{\rm isotropic} = I_{E\|a} + I_{E\|b} + I_{E\|c}$, of

TABLE I. The J_z coefficients α_{J_z} and β_{J_z} describing the wave functions of the crystal-field GS Kramer's doublets for solution No. 1. The wave functions have been calculated with the full multiplet routine, using c as the quantization axis.

$\lvert J,J_z\rangle$	|GS#1⟩ $CeOs_2Al_{10}$	|GS#1⟩ $CeFe_2Al_{10}$
$\lvert 5/2,\pm 5/2\rangle$	$\pm 0.48(2)$	$\pm 0.44(2)$
$\lvert 5/2,\pm 1/2\rangle$	$\pm 0.27(2)$	$\pm 0.15(2)$
$\lvert 5/2,\mp 3/2\rangle$	$\pm 0.83(2)$	$\pm 0.88(2)$
$\lvert 7/2,\pm 5/2\rangle$	$\mp 0.06(1)$	$\mp 0.07(1)$
$\lvert 7/2,\pm 1/2\rangle$	$\pm 0.00(1)$	$\pm 0.01(1)$
$\lvert 7/2,\mp 3/2\rangle$	$\mp 0.04(1)$	$\mp 0.03(1)$
$\lvert 7/2,\mp 7/2\rangle$	$\pm 0.02(1)$	$\pm 0.01(1)$

TABLE II. Crystal-field parameters $\check{A}^m_k$ in meV from full multiplet calculations. For definition and conversion to Stevens parameters B^m_k see Ref. 35. Note that Stevens parameters by definition do not include the $J = 7/2$ contributions to the wave functions listed in Table I.

|GS#1⟩	$\check{A}^0_2$	$\check{A}^2_2$	$\check{A}^0_4$	$\check{A}^2_4$	$\check{A}^4_4$
$CeOs_2Al_{10}$	42(5)	44(2)	160(8)	3(10)	−81(4)
$CeFe_2Al_{10}$	4(8)	19(2)	154(5)	7(10)	−103(5)

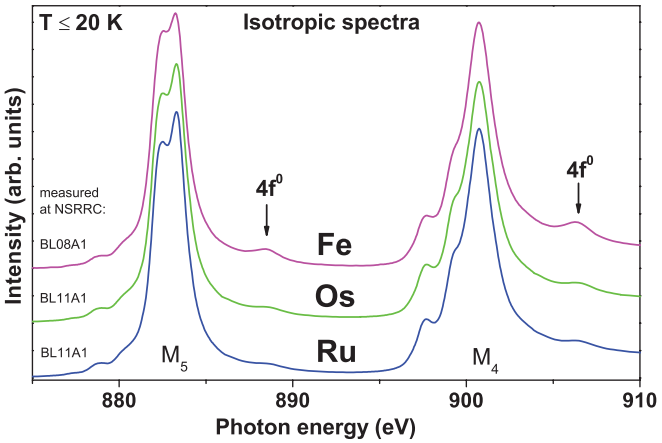

FIG. 3. (Color online) Experimental isotropic low-temperature x-ray absorption spectra $I_{\text{isotropic}} = I_{E\|a} + I_{E\|b} + I_{E\|c}$ of $CeRu_2Al_{10}$, $CeOs_2Al_{10}$, and $CeFe_2Al_{10}$ at the $M_{4,5}$ absorption edge. The arrows mark the absorption intensities due to the $4f^0$ contribution in the ground state.

the three compounds $CeRu_2Al_{10}$, $CeOs_2Al_{10}$, and $CeFe_2Al_{10}$. There are two strong absorption edges due to the transitions $3d^{10}4f^1 \rightarrow 3d^9_{5/2}4f^2$ (M_5) and $3d^{10}4f^1 \rightarrow 3d^9_{3/2}4f^2$ (M_4), and in addition some small humps at about 888 and 906 eV (see arrows) which are due to the $4f^0$ contribution in the ground state. The $4f^0$ amount is very small in $CeRu_2Al_{10}$, only slightly increased in the Os sample, but rather pronounced in the Fe compound. The $4f^0$ contribution increases relatively as 1 to 1.4 to 3.8 from Ru to Os, and Fe. Here the f^0 amounts have been determined by integration over the range of the $4f^0$ humps after subtracting a linear background (see Ref. 42). This trend agrees with findings from static susceptibility, i.e., that the c-f hybridization increases from M = Ru to Os and is largest for Fe.

We have shown that the c-f hybridization is reflected in the XAS data as small $4f^0$ spectral weights. Hence, the question arises whether the presence of some $4f^0$ contribution in the ground state has an impact on the validity of the CEF-only interpretation. Here the temperature dependence of the linear dichroism can give further insight. Figure 4 shows the M_5 edge of the Os and Fe compound for several temperatures. For reasons of clarity only two polarizations are shown. The magnetic ordering and Kondo temperatures as estimated from the maximum in the static susceptibility [$T_K \approx 3T_{\max}$ of $\chi_a(T)$] are marked with red arrows. For the Os sample the polarization shows no temperature effect below 150 K, i.e., as in $CeRu_2Al_{10}$ neither the magnetic ordering transition nor the spin gap has an impact on the polarization. Only for $T \geqslant 150$ K the polarization decreases slightly. When cooling again below 150 K the polarization recovers.

The absence of a temperature effect across the magnetic ordering transition has been reported previously.[35,42] It can be understood when considering that the Zeeman splitting of the Kramer's doublets due to the magnetic order is small with respect to the large CEF splittings. Consequently the two states of the Kramer's doublets remain unchanged. Moreover, the two states of a Kramer's doublet are identical so that they give rise to the same LD. The slight change of LD in the $CeOs_2Al_{10}$ data when warming up from 100 to 150 K can be understood

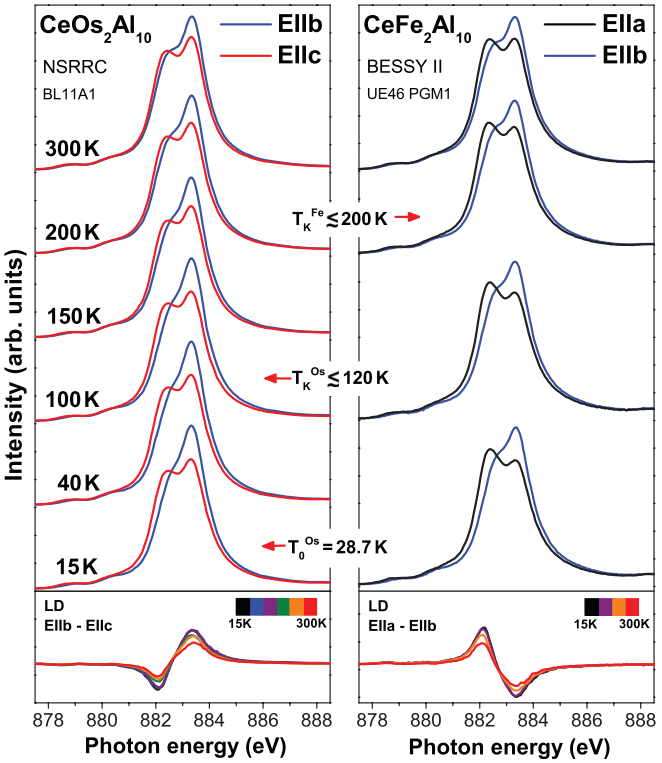

FIG. 4. (Color online) Measured temperature-dependent x-ray absorption spectra of $CeOs_2Al_{10}$ (left) and $CeFe_2Al_{10}$ (right) at the M_5 edge. The bottom panels show the respective LD for each temperature. The magnetic ordering and Kondo temperatures as estimated from the maximum in the static susceptibility along the crystallographic a axis $\chi_a(T)$ ($T_K \lesssim 3\,T_{\max}$) are marked with red arrows.

in two ways: At 150 K the population of the first excited CEF level at 38 meV amounts to ∼5 %, i.e., the change in the LD could be purely explained by the population of an excited CEF state. However, if the variation of the LD was due to the Kondo effect or a mixture of Kondo and the population of a higher state, how large would be the mistake by applying a CEF-only analysis? At 150 K the system is in the single ion regime and through thermal population the first excited CEF state contributes ∼5 % to the signal. Consequently the 150 K data contain 95% of the CEF ground-state anisotropy. This sets an upper limit for the mistake caused by ignoring the c-f hybridization in the simulation of the low-temperature data. Also in the Fe compound the population of the excited CEF levels could account for the temperature dependence of the polarization. However, following the same line of thought as for Os we find that the 200 K data ($T \geqslant T_K$) contain 90% of the ground-state polarization. We are still able to describe the low-temperature anisotropy in terms of a CEF-only model, although the potential error due to neglecting the hybridization is larger than for $CeOs_2Al_{10}$.

We note that for the present compounds linearly polarized soft XAS is able to describe the initial state symmetry in terms of a CEF model despite the presence of a strong Kondo effect. This is in contrast to INS, where the magnetic excitations suffer from strong intrinsic broadening due to strong c-f hybridization such that it becomes hard to separate CEF excitations from the strong phonon background. For

the present class of compounds the spin gap aggravates the problem to determine wave functions from the relative spectral weights of the magnetic quasi- and inelastic scattering in the INS data. Hence soft XAS is a very useful complementary method.

To summarize, we are able to give CEF GS wave functions for the two orthorhombic Kondo insulators $CeOs_2Al_{10}$ and $CeFe_2Al_{10}$ from a combined analysis of linearly polarized soft XAS and static susceptibility data.[5,32] The analysis is not hampered by the spin gaps which have been found in INS, and the CEF description can be applied despite the strong c-f hybridization in these compounds. In $CeOs_2Al_{10}$ the small ordered moment along the c direction can be explained with CEF effects only, something we also found for $CeRu_2Al_{10}$.[35] However, the difference between the CEF-only moment and the actual ordered moment might well be due to Kondo screening.

We thank D. T. Adroja for providing the unpublished CEF energies of $CeOs_2Al_{10}$ and $CeFe_2Al_{10}$. This work was supported by Deutsche Forschungsgemeinschaft Grant No. 583872, Germany and KAKENHI No. 20102004 of MEXT, Japan.

[1] A. M. Strydom, Physica B **404**, 2981 (2009).
[2] T. Nishioka, Y. Kawamura, T. Takesaka, R. Kobayashi, H. Kato, M. Matsumura, K. Kodama, K. Matsubayashi, and Y. Uwatoko, J. Phys. Soc. Jpn. **78**, 123705 (2009).
[3] K. Hanzawa, J. Phys. Soc. Jpn. **79**, 043710 (2010).
[4] S. Kambe, H. Chudo, Y. Tokunaga, T. Koyama, H. Sakai, T. U. Ito, K. Ninomiya, W. Higemoto, T. Takesaka, T. Nishioka, and Y. Miyake, J. Phys. Soc. Jpn. **79**, 053708 (2010).
[5] Y. Muro, J. Kajino, K. Umeo, K. Nishimoto, R. Tamura, and T. Takabatake, Phys. Rev. B **81**, 214401 (2010).
[6] T. Takesaka, K. Oe, R. Kobayashi, Y. Kawamura, T. Nishioka, H. Kato, M. Matsumura, and K. Kodama, J. Phys.: Conf. Ser. **200**, 012201 (2010). (Note: Here a different labeling of the crystallographic axes in the susceptibility of $CeFe_2Al_{10}$ has been used.)
[7] C. S. Lue, S. H. Yang, A. C. Abhyankar, Y. D. Hsu, H. T. Hong, and Y. K. Kuo, Phys. Rev. B **82**, 045111 (2010).
[8] H. Tanida, D. Tanaka, M. Sera, C. Moriyoshi, Y. Kuroiwa, T. Takesaka, T. Nishioka, H. Kato, and M. Matsumura, J. Phys. Soc. Jpn. **79**, 083701 (2010).
[9] J. Robert, J.-M. Mignot, G. André, T. Nishioka, R. Kobayashi, M. Matsumura, H. Tanida, D. Tanaka, and M. Sera, Phys. Rev. B **82**, 100404(R) (2010).
[10] D. D. Khalyavin, A. D. Hillier, D. T. Adroja, A. M. Strydom, P. Manuel, L. C. Chapon, P. Peratheepan, K. Knight, P. Deen, C. Ritter, Y. Muro, and T. Takabatake, Phys. Rev. B **82**, 100405 (2010).
[11] D. T. Adroja, A. D. Hillier, P. P. Deen, A. M. Strydom, Y. Muro, J. Kajino, W. A. Kockelmann, T. Takabatake, V. K. Anand, J. R. Stewart, and J. Taylor, Phys. Rev. B **82**, 104405 (2010).
[12] C. S. Lue, S. H. Yang, T. H. Su, and B.-L. Young, Phys. Rev. B **82**, 195129 (2010).
[13] A. Kondo, J. Wang, K. Kindo, T. Takesaka, Y. Ogane, Y. Kawamura, T. Nishioka, D. Tanaka, H. Tanida, and M. Sera, J. Phys. Soc. Jpn. **80**, 013701 (2011).
[14] S.-I. Kimura, T. Iizuka, H. Miyazaki, A. Irizawa, Y. Muro, and T. Takabatake, Phys. Rev. Lett. **106**, 056404 (2011).
[15] K. Hanzawa, J. Phys. Soc. Jpn. **80**, 023707 (2011). (Note: Hanzawa uses the b axis as the quantization axis.)
[16] A. Kondo, J. Wang, K. Kindo, Y. Ogane, Y. Kawamura, S. Tanimoto, T. Nishioka, D. Tanaka, H. Tanida, and M. Sera, Phys. Rev. B **83**, 180415 (2011).
[17] H. Kato, R. Kobayashi, T. Takesaka, T. Nishioka, M. Matsumura, K. Kaneko, and N. Metoki, J. Phys. Soc. Jpn. **80**, 073701 (2011).
[18] M. Matsumura, H. Tanida, D. Tanaka, H. Kato, T. Nishioka, and M. Sera, J. Phys. Soc. Jpn. **80**, 085001 (2011).
[19] K. Yutani, Y. Muro, J. Kajino, T. J. Sato, and T. Takabatake, J. Phys.: Conf. Ser. **391**, 012070 (2012).
[20] K. Hanzawa, J. Phys. Soc. Jpn. **80**, 113701 (2011).
[21] S.-I. Kimura, T. Iizuka, H. Miyazaki, T. Hajiri, M. Matsunami, T. Mori, A. Irizawa, Y. Muro, J. Kajino, and T. Takabatake, Phys. Rev. B **84**, 165125 (2011).
[22] H. Tanida, D. Tanaka, Y. Nonaka, M. Sera, M. Matsumura, and T. Nishioka, Phys. Rev. B **84**, 233202 (2011).
[23] J. Goraus and A. Slebarski, J. Phys.: Condens. Matter **24**, 095503 (2012).
[24] H. Tanida, Y. Nonaka, D. Tanaka, M. Sera, Y. Kawamura, Y. Uwatoko, T. Nishioka, and M. Matsumura, Phys. Rev. B **85**, 205208 (2012).
[25] C. S. Lue, H. F. Liu, B. D. Ingale, J. N. Li, and Y. K. Kuo, Phys. Rev. B **85**, 245116 (2012).
[26] J. Robert, J.-M. Mignot, S. Petit, P. Steffens, T. Nishioka, R. Kobayashi, M. Matsumura, H. Tanida, D. Tanaka, and M. Sera, Phys. Rev. Lett. **109**, 267208 (2012).
[27] Y. Muro, K. Motoya, Y. Saiga, and T. Takabatake, J. Phys. Soc. Jpn. **78**, 083707 (2009).
[28] Y. Muro, K. Motoya, Y. Saiga, and T. Takabatake, J. Phys.: Conf. Ser. **200**, 012136 (2010).
[29] S. C. Chen and C. S. Lue, Phys. Rev. B **81**, 075113 (2010).
[30] Y. Kawamura, S. Edamoto, T. Takesaka, T. Nishioka, H. Kato, M. Matsumura, Y. Tokunaga, S. Kambe, and H. Yasuoka, J. Phys. Soc. Jpn. **79**, 103701 (2010).
[31] S.-I. Kimura, Y. Muro, and T. Takabatake, J. Phys. Soc. Jpn. **80**, 033702 (2011).
[32] Y. Muro, K. Yutani, J. Kajino, T. Onimaru, and T. Takabatake, J. Korean Phys. Soc. (to be published).
[33] V. Thiede, T. Ebel, and W. Jeitschko, J. Mater. Chem. **8**, 125 (1998).
[34] A. I. Tursina, S. N. Nesterenko, E. V. Murashova, I. V. Chernyshev, H. Noël, and Y. D. Seropegin, Acta Crystallogr. Sect. E: Struct. Rep. Online **61**, i12 (2005).
[35] F. Strigari, T. Willers, Y. Muro, K. Yutani, T. Takabatake, Z. Hu, Y.-Y. Chin, S. Agrestini, H.-J. Lin, C. T. Chen, A. Tanaka, M. W. Haverkort, L.-H. Tjeng, and A. Severing, Phys. Rev. B **86**, 081105(R) (2012).
[36] J. C. Fuggle, F. U. Hillebrecht, J.-M. Esteva, R. C. Karnatak, O. Gunnarsson, and K. Schönhammer, Phys. Rev. B **27**, 4637 (1983).
[37] G. Kaindl, G. Kalkowski, W. D. Brewer, B. Perscheid, and F. Holtzberg, J. Appl. Phys. **55**, 1910 (1984).
[38] A. Tanaka and T. Jo, J. Phys. Soc. Jpn. **63**, 2788 (1994).

[39]P. Hansmann, A. Severing, Z. Hu, M. W. Haverkort, C. F. Chang, S. Klein, A. Tanaka, H. H. Hsieh, H.-J. Lin, C. T. Chen, B. Fåk, P. Lejay, and L. H. Tjeng, Phys. Rev. Lett. **100**, 066405 (2008).
[40]D. T. Adroja (private communication).
[41]M. W. Haverkort (private communication).
[42]T. Willers, D. T. Adroja, B. D. Rainford, Z. Hu, N. Hollmann, P. O. Körner, Y.-Y. Chin, D. Schmitz, H. H. Hsieh, H.-J. Lin, C. T. Chen, E. D. Bauer, J. L. Sarrao, K. J. McClellan, D. Byler, C. Geibel, F. Steglich, H. Aoki, P. Lejay, A. Tanaka, L. H. Tjeng, and A. Severing, Phys. Rev. B **85**, 035117 (2012).